

# Numerical Investigation of Storage Behaviors of A Liquid CO<sub>2</sub> Tank

Yu Weng<sup>1</sup>, Liang Li<sup>2</sup>, Xia Liu<sup>2</sup>, Libo Cheng<sup>3</sup>, Yongchun Liu<sup>3</sup>, Shuang Yang<sup>4</sup>

<sup>1</sup> College of Petroleum Engineering, Xi'an Shiyou University Shaanxi Province Aerospace and Astronautics Propulsion Research Institute Xi'an, Shaanxi, China

<sup>2</sup> Shaanxi Province Aerospace and Astronautics Propulsion Research Institute Xi'an, Shaanxi, China

<sup>3</sup> Shaanxi Aerospace Supercomputing Center Co., Ltd. Xi'an, Shaanxi, China

<sup>4</sup> College of Petroleum Engineering, Xi'an Shiyou University Xi'an, Shaanxi, China

**Abstract.** The dynamic behavior of heat transfer induced by flow of the storage tank during the storage process was investigated using the computational fluid dynamics (CFD) approach, with the target of the liquid CO<sub>2</sub> storage tank in a CO<sub>2</sub> injection station in an oilfield. The flow field distribution outside the tank was simulated, exhibiting the patterns of air flow near the tank wall. The effect of progressive cooling leakage in the tank under various conditions was determined through simulation of the dynamic of flow heat transfer under various storage settings, with the result indicating that tank pressure has a beneficial effect on cooling capacity. The medium level, on the other hand, had a negative impact on cooling capacity. Finally, the impact of environmental variables on fluid loss was evaluated. This finding supports the safety and cost-benefit analysis of liquid CO<sub>2</sub> storage systems.

**Keywords:** liquid CO<sub>2</sub>, computational fluid dynamics, cryogenic storage tank, dynamic behavior

## 1. Introduction

With the development of CO<sub>2</sub> research in recent years in countries all over the world, CO<sub>2</sub> capture, and storage technology has also developed significantly, and Enhanced oil recovery (EOR) technology has been widely explored and adopted. By injecting a little amount of CO<sub>2</sub> into the geological structure, not only may a large amount of CO<sub>2</sub> be stored underground, but oil well recovery can also be enhanced. CO<sub>2</sub> is commonly stored in low-temperature liquefaction in application scenarios. The storage tank would continually absorb heat from the environment outside the storage tank since the continuous storage temperature of CO<sub>2</sub> in the storage tank is much lower than the temperature outside the storage tank. Consequently, the temperature in the storage tank of CO<sub>2</sub> rises, and the pressure rises as well. Once the gas pressure in the storage tank exceeds the threshold safety value, the safety valve opens automatically, releasing a small amount of gas from the storage tank and lowering the pressure value in the storage tank, however CO<sub>2</sub> discharged from the storage tank does not. While diminishing the storage tank's liquid storage capacity, it also has a negative impact on the environment. To this reason, it is required to investigate CO<sub>2</sub> storage features[1,2].

Previous research has given us with a wealth of theoretical evidence[3,4], but the works mentioned above are primarily concerned with theoretical analysis and scaling

experiments. There are few studies on entire storage tank dynamic storage properties, and even fewer studies on CO<sub>2</sub>. Based on a CO<sub>2</sub> flooding pilot test conducted in an oil field, this study examines the dynamic of the storage process of the liquid CO<sub>2</sub> storage tank, to assure the safety and economy of the liquid CO<sub>2</sub> storage system.

## 2. Method

### 2.1 Governing equations

For the dynamic storage studies of storage tanks, three-dimensional computational fluid dynamics (CFD) method was used and its governing equations include: mass, momentum and energy conservation equation. The details are as follows:

$$\frac{\partial}{\partial t}(\rho) + \nabla \cdot \vec{u} = 0 \quad (1)$$

$$\frac{\partial}{\partial t}(\rho u) + \nabla \cdot (\rho u_i u) = \nabla \cdot (\mu \cdot \text{grad} u_i) - \nabla p + S_i \quad (2)$$

$$\frac{\partial}{\partial t}(\rho T) + \text{div}(\rho u T) = \text{div} \left( \frac{k}{c_p} \text{grad} T \right) + S_T \quad (3)$$

Where:  $\vec{u}$  is velocity vector,  $S$  is source item,  $S_T$  is viscous dissipative item.

The VOF model based on phase interface tracking technology is applied to simulate the gas-liquid two-phase problem in the storage tank [5,6].

The phase change mass transfer model suggested by Lee is used to simulate the condensation or boiling mass transfer problem in the storage tank [7]:

$$\begin{cases} S_{aq} = -r \cdot a_l \rho_l \frac{T - T_s}{T_s}, & T \geq T_s \\ S_{aq} = r \cdot a_g \rho_g \frac{T_s - T}{T_s}, & T < T_s \end{cases} \quad (4)$$

Where,  $r$  is heat transfer coefficient during phase transition, the subscripts  $l$  and  $g$  are the liquid and gas phases, respectively,  $T_s$  is Saturation temperature of each phase.

## 2.2 Storage Tank details

In the injection station, a horizontal cryogenic liquid storage tank with an effective volume of 50m<sup>3</sup> is used. Figure 1 presents the injection station's site. The storage tank is built with a double-layer metal tank body and a vacuum powder insulating layer as the interlayer. The storage tank's design pressure is 2.84MPa, and its geometric volume is 52m<sup>3</sup>. Figure 2 shows the structure of storage tank.

The operational settings of the storage tank in the test injection station vary widely to assist the test. The analysis conditions are determined based on the field investigation, in order to accurately study the influence of each parameter on the dynamic of storage process. The comparison of storage performance in this study is based on the following benchmark requirements: The tank's pressure is 2.4 MPa, the ambient temperature is 20°C, and the wind speed is 0 m/s.



Fig.1 Test injection station scene diagram

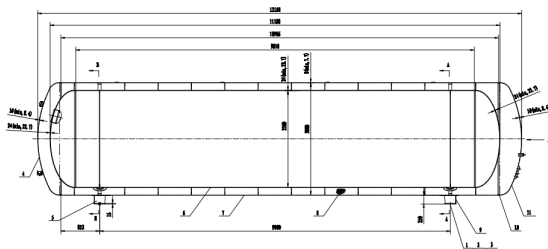


Fig.2 Structural drawing of storage tank

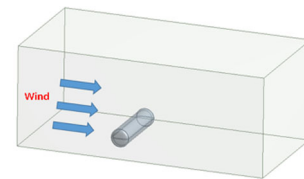
According to the layout diagram of the reinjection system, combined with the on-site measurement, the overall 3D model is constructed as shown in Figure 2.

## 2.3 Geometry and mesh details

The scouring of the tank wall by ambient air flow in a horizontal storage tank is not fully uniform in practice, and there are variances between the windward and leeward sides. To account for this unequal distribution, our research developed an analytical model that included

outer space (see Fig. 3). (a). A substantial thermal insulation layer is also created between the inner and outer tanks of the storage tank to imitate the storage tank's thermal insulation capacity. Figure 3 shows a three-dimensional model of the storage tank (b).

The total analytical model was partitioned geometrically using a polyhedral mesh, yielding a mesh model with around 3.2 million elements. Figure 3 illustrates the local mesh model (c). The tank's medium is pure CO<sub>2</sub>, and the physical characteristics are taken from the National Institute of Standards and Technology (NIST) [8,9]. The dynamic process is computed using the transient time advance method in under 24 hours under various initial storage conditions.



(a) Geometric model of overall modelling and layout



(b) The mesh details of storage tank

Fig.3 Geometry and mesh details

## 3. Results And Discussion

### 3.1 Dynamic behavior of storage process

Figure 4 shows the distribution of the air flow field outside the tank using a wind speed of 23 m/s as an example. The windward side of the storage tank shows an evident cylindrical flow distribution, with relatively strong surface shear wind speeds at the top and bottom. There is visible flow separation on the leeward side, and low-speed vortices of various scales are isolated from the tank, resulting in a reduction in shear wind speed on the leeward side. The temperature distribution of the tank wall after 2 hours of storage (as shown in Figure 6) shows that the temperature on the windward side of the tank wall is generally higher than that on the leeward side, and the heads at both ends are generally higher than the barrel body, both of which are affected by the flow field.

After 2 hours of storage, Figure 7 depicts the velocity distribution in the tank. The presence of a natural convection phenomenon in the tank can be seen. The liquid in the tank circulates at a low speed due to heat transfer from the tank wall. The convective velocity of the gas in the upper part of the tank is higher than that of the liquid, due to the significant changing in gas density with temperature.

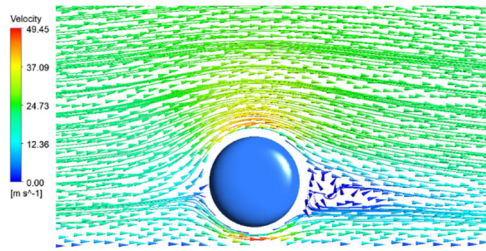
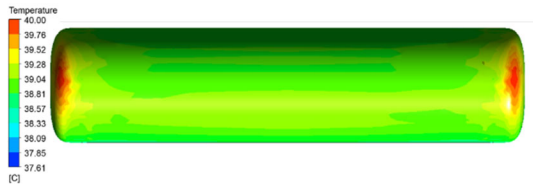
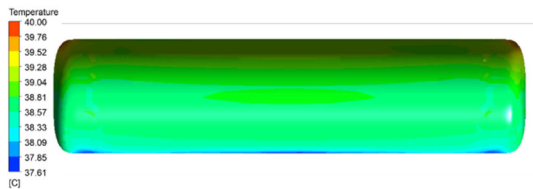


Fig.4 Velocity spectrum of outlet pipe of reinjection pump



(a) The windward side of the outer wall of the tank



(b) The top surface of tank

Fig.5 Acceleration Spectrum of Outlet Tube of Reinjection Pump

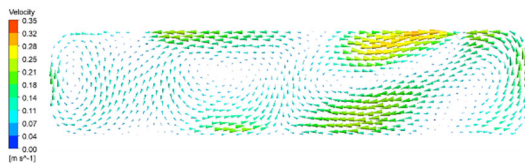


Fig.6 Velocity vector distribution in tank

### 3.2 The effect of storage conditions

The tank conditions have a considerable impact on the overall cooling leakage for the first storage circumstances, within 24 hours. The lower the tank pressure, the larger the amount of cold that leaks out. According to the quantitative investigation, under extreme conditions (1.9MPa), a liquid loss of around 0.035 percent can be generated while the tank pressure is increased by 0.4MPa. It can be shown that increasing the storage pressure reduces evaporation loss to a certain extent.

Due to the nonlinear relationship between the starting liquid level and the liquid volume in the tank, it can be calculated that the initial liquid level in a given range (around 0.75m) results in more liquid evaporation loss than the initial liquid level outside of this range. Then the liquid evaporation loss reduces steadily, and it's surprising to see that a liquid level of 0.75m might result in 30 times the loss compared to a full tank (2.3m). Avoiding storage around medium liquid levels reduces evaporation losses significantly.

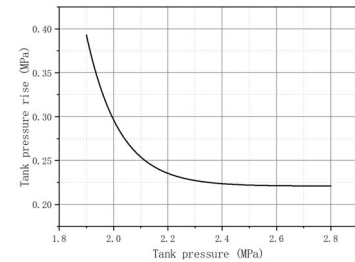
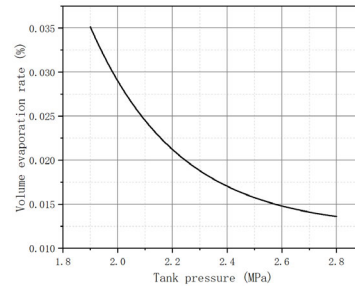


Fig.7 Effect of initial tank pressure on storage characteristics in a single day (a) Volume evaporation rate (b) Tank pressure rise

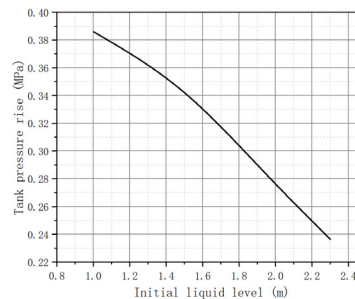
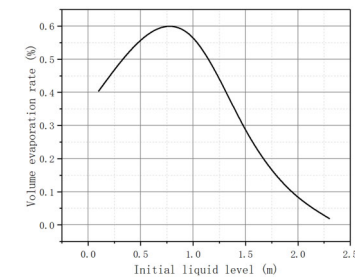


Fig.8 Effect of initial liquid level on storage characteristics in a single day (a) Volume evaporation rate (b) Tank pressure rise

### 3.3 The effect of environmental conditions

For the environmental conditions (temperature, wind speed), simulation results show that as the temperature or speed of air flow rises, evaporation loss rises, and tank pressure goes up. In addition, there is obvious evaporation in the tank during storage under extreme weather conditions, which can result in constant liquid loss. It's worth mentioning that in extreme cases, it could result in 0.063 percent liquid loss and a 0.66MPa rise in tank pressure.

Furthermore, the influence of ambient temperature on evaporation and tank pressure rise is much greater than that of wind speed in the case studied in this paper. This is owing to the fact that thermal conduction losses are higher in double-layer insulated tanks than convective heat losses.

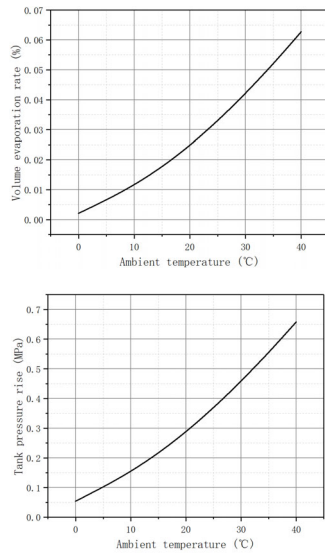


Fig.9 Effect of ambient temperature on storage characteristics in a single day (a) Volume evaporation rate (b) Tank pressure rise

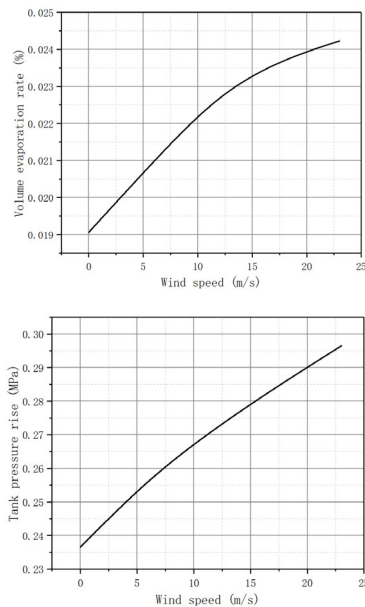


Fig.10 Effect of wind speed on storage characteristics in a single day (a) Volume evaporation rate (b) Tank pressure rise

## 4. Conclusions

In this work, the dynamic behaviors of heat transfer induced by air flow of the storage tank during the storage process was analyzed and evaluated using the CFD approach, utilizing the liquid CO<sub>2</sub> storage tank in a CO<sub>2</sub> injection station in an oilfield as a base case. The key conclusions obtained are as follows:

(1) An analytical model was established, which includes external space, a double-layer tank, and tank space, and faithfully represents the storage tank's actual operating environment.

(2) Based on the VOF model of phase interface tracking technology, a numerical analysis method and physical model considering complete flow, heat transfer, and phase transition were established;

(3) The influence of gradual cooling leakage in the tank under different conditions was revealed by simulating the dynamic behavior of flow and heat transfer under varied storage conditions. Furthermore, the role of tank pressure on cooling capacity is determined to be beneficial, as is the effect of medium level on cooling detrimental effects of ability. It's worth noting that when the weather (temperature, wind speed) is terrible, there's a lot of evaporation in the tank during storage, which can lead to constant liquid loss.

## Acknowledgment

This work was financially supported by the Natural Science Basic Research Program of Shaanxi (Program No. 2021JM-402), and Key Research and Development Program of Shaanxi (Program No. 2022ZDLGY02-06).

## References

1. Havens, J., et al. "Characterization of the LGFSTF Wind Tunnel in Preparation for the DOE/EPA Hazardous Chemical Evaporation Rate Experiments." Office of Scientific & Technical Information Technical Reports, 1995.
2. Gerbec, M., et al. "A Comparison of Dispersion Models for the LNG Dispersion at Port of Koper, Slovenia." *Safety Science*, vol. 144, no. 3, 2021, p. 105467.
3. Ping, W., et al. "Measurement and Calculation of Cryogenic Thermal Conductivity of HGMs." *International Journal of Heat and Mass Transfer*, vol. 129, 2018, pp. 591–98.
4. Jeon, S. J., et al. "Design Feature of Large Full Containment LNG Storage Tank." 2010 AIChE Spring National Meeting, 2010.
5. Cummins, Brian M., et al. "Time-Dependent Model for Fluid Flow in Porous Materials with Multiple Pore Sizes." *Analytical Chemistry*, vol. 89, no. 8, 2017, pp. 4377–81.
6. Walters, D. K., and N. M. Wolgemuth. "A New Interface-Capturing Discretization Scheme for Numerical Solution of the Volume Fraction Equation in Two-Phase Flows." *International Journal for Numerical Methods in Fluids*, vol. 60, no. 8, 2010, pp. 893–918.
7. Sholl, C. A., and N. H. Fletcher. "Decoration Criteria for Surface Steps." *Acta Metallurgica*, vol. 18, no. 10, 1970, pp. 1083–86.
8. Clementoni, E. M., and T. L. Cox. "Comparison of Carbon Dioxide Property Measurements for an Operating Supercritical Brayton Cycle to the REFPROP Physical Property Database." *Asme Turbo Expo: Turbine Technical Conference & Exposition*, 2014.
9. Lemmon, E. W., et al. "NIST Standard Reference Database 23: Reference Fluid Thermodynamic and Transport Properties-REFPROP. 9.0." NIST NSRDS -, 2010.